Anticipated Transient Without Scram in the PB-FHR: Review and Proposal

Kathryn D. Huff
Xin Wang

Contents

When licensing a novel reactor technology, regulatory bodies such as the Nuclear Regulatory Commission (NRC) require robust analysis of reactor performance during Design Basis Events (DBEs) and Beyond Design Basis Events (BDBEs). By definition, design decisions are not primarily driven by BDBEs. However, detailed analysis of BDBEs may inform design decisions that improve reactor response to catastrophic events. These analyses may even illuminate design decisions which could increase the feasibility of reactor restart after such an event.

The following describes the scope of analysis necessary to characterize the response of the a novel reactor technology to various BDBEs in the context of design decisions. In particular, this work will focus on reactor system response to Anticipated Transient Without Scram (ATWS) scenarios in the Pebble-Bed Fluoride-Salt-Cooled High-Temperature Reactor (PB-FHR). These scenarios include Loss of Heat Sink (LOHS), Loss of Forced Cooling (LOFC), and Loss of Large Area (LOLA) incidents, among others. Additionally, reactor response to intentional reactivity instertions and Reactivity Insertion Accidents (RIAs) will be considered.

For background and context, ATWS scenarios being considered will first be described and specific relevant features of the PB-FHR will be mentioned.

Temporal and spatial coupling between a transient thermal-hydraulics model and transient neutronics model will be necessary for high confidence in transient behavior in the PB-FHR. As a review, typical methods of transient neutronic and thermal-hydraulics coupling will be described and the importance of multiphysics coupling will be explored with particular emphasis on the tools proposed for future use.

Next, previous work related to coupled thermal-hydraulics and neutronics behavior, both steady state and transient, in this and similar reactor designs will next reviewed. Current work utilizing loosely coupled steady state assessments to determine beginning and end of transient temperatures will also be mentioned.

Finally, a proposed outline for future work will be described. This proposal will emphasize building upon previous work by utilizing existing special purpose tools as well as proposing specific benchmark activities to be confirm results in relation to other tools and previous analyses.

1 Background

The response of the Mark 1 PB-FHR core to ATWS is an area of interest as the design process proceeds. In particular, this analysis is concerned with the extent to which an PB-FHR ATWS may cause damage to components due to high power densities, fuel temperatures, and resulting outlet coolant temperature evolution to which metallic components outside of the core are exposed. This is especially important since, for the PB-FHR, the time at which metallic components are exposed to high temperatures is likely to dominate structural integrity limitations [2].

1.a Anticipated Transient Without Scram

For licensing a novel reactor technology, regulatory bodies such as the NRC require robust analysis of DBEs and BDBEs. A key BDBE for the PB-FHR is an ATWS. A number of initiating events can result in an ATWS. Categories of such events include LOFC, LOHS, and LOLA scenarios. In addition, BDBE sequences resulting from an intentional reactivity insertion or a RIA are of interest. The following sections describe those scenarios.

1.a.1 Loss of Forced Cooling

In a LOFC scenario, forced coolant circulation ceases. This may occur due to a station blackout and loss of backup power resulting in pump failure. Forced circulation in the PB-FHR is provided by pumps that provide a total pumping power that is currently a design parameter. When forced coolant circulation is lost, natural circulation inherent in the PB-FHR Mark 1 design continues to circulate the coolant, though at a lower rate than ordinary operation. The reduced flow will reduce the heat removal effectiveness of the coolant, introducing a temperature transient in the coolant and fuel.

$$v_{cool}(t) = v_{nat} + (1 - H(t_0))v_{pp} \tag{1}$$

where

$$v_{cool}(t) = \text{coolant velocity } [m/s] \tag{2}$$
$$v_{nat} = \text{velocity from natural circulation } [m/s] \tag{3}$$
$$v_{pp} = \text{velocity from pumping power } [m/s] \tag{4}$$
$$H(t) = \text{Heaviside Step Function} \tag{5}$$
$$t_0 = \text{Time of pump shutoff} \tag{6}$$

1.a.2 Loss of Heat Sink

In a LOHS scenario, there is full failure of ordinary heat removal. This scenario results in excess heating power in the fuel, coolant, reflector, and other reactor components. Heat removal in the PB-FHR is ordinarily provided by the Coiled Tube Air Heaters (CTAHs) as well as the Direct Reactor Auxiliary Cooling System (DRACS) system. If the function of one or both of these are lost, the progression of the accident sequence will result in heightened coolant temperature followed by a resulting power transient and possible instabilities.

$$T_{cool,in}(t) = T_{cool,out} - (1 - H(t_0))\Delta T_{hs} \tag{7}$$

where

$$T_{cool,in}(t) = \text{coolant temperature at inlet } [K] \tag{8}$$
$$T_{cool,out} = \text{coolant temperature at outlet } [K] \tag{9}$$
$$\Delta T_{hs} = \text{change in temperature from heat sink system } [K] \tag{10}$$
$$H(t) = \text{Heaviside Step Function} \tag{11}$$
$$t_0 = \text{Time at loss of heat sink} \tag{12}$$

1.a.3 Loss of Large Area

In a LOLA scenario, such as a tsunami or other catastrophic event, many systems are assumed to fail simultaneously and catastrophically. In such a scenario both LOFC and LOHS are assumed to occur simultaneously. For the PB-FHR, the combined effects of these failures may balance each other, as has been seen in other novel reactors such as the High Temperature Gas Reactor (HTGR).

1.a.4 Reactivity Insertion

Reactivity insertion is induced when a control rod or many are removed from the core, introducing a sudden positive reactivity. Since the buoyantly driven control rods and blades enter the core when their control drives fail, the reactor design must be modified before a reactivity insertion is possible. Therefore, in the PB-FHR, reactivity insertion must be intentional, as the rods or blades must be rapidly removed intentionally with the safety mechanisms either modified for pulsed behavior or nefariously disrupted.

Since the amount of disruption necessary is high, a nefarious party is unlikely to cause an RIA. However, depending on the robustness of the PB-FHR against reactivity insertion, the operators may intentionally insert reactivity for pulsed flux experiments.

$$\rho_{ext}(t) = f(t) \tag{13}$$

where

$$\rho_{ext} = \text{externally inserted reactivity } [pcm] \tag{14}$$
$$f(t) = \text{arbitrary reactivity insertion function } [pcm] \tag{15}$$
$$\tag{16}$$

In this case, temperature responds to reactivity increases and power generated in the fuel then propagates to the coolant and components.

1.b Relevant Features of the PB-FHR

The Mark 1 PB-FHR is a novel reator design that utilizes annular pebble fuel, Fluoride-Lithium-Beryllium (FLiBe) salt coolant. For moderation, the annular core design wraps around a central solid graphite reflector. The fuel pebbles in the core annulus are surrounded by an outer layer of graphite reflector pebbles as well as a cylindrical outer graphite reflector block.

1.b.1 TRISO Pebble Fuel

Gently buoyant fuel pebbles circulate continuously from the bottom to the top of the PB-FHR design. The pebble fuel in the PB-FHR is 3 cm in diameter and is multiply heterogeneous. A low density graphite core is surrounded by a fuel matrix of microscopic Tristructural Isotropic (TRISO) fuel particles. That annular fuel matrix is in turn surrounded by a high density graphite shell. Figure 1 demonstrates the multiple heterogeneities of this pebble fuel design.

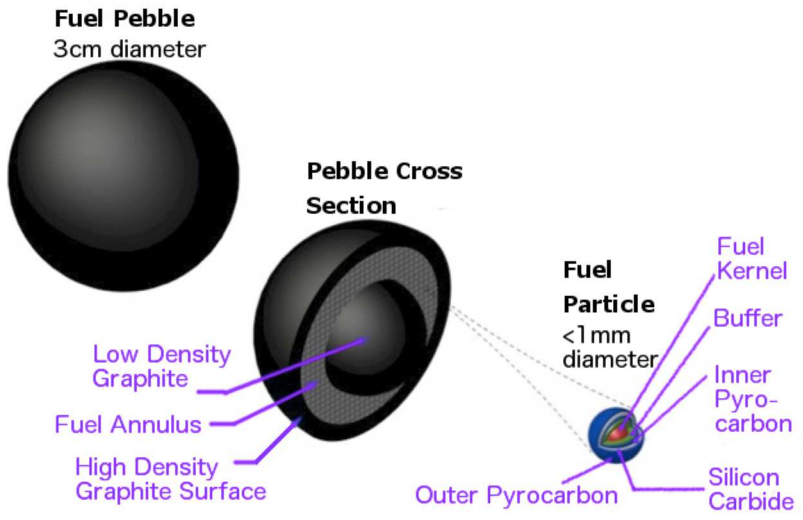

Figure 1: The PB-FHR fuel pebbles demonstrate multiple heterogeneities [3].

The proximity of the fuel matrix to the coolant increases heat removal from the fuel and flattens the temperature profile accross the pebble, increasing safety margin during transients.

1.b.2 FLiBe Salt

The coolant in this reactor is a Fluoride-Lithium-Beryllium salt. This salt is a high viscosity, high Prandtl number liquid for an enormous window of temperatures. With a melting point of $459.1°C$ and a boiling point of $1430°C$, even the highest accident temperatures are unlikely to boil the coolant. Therefore, the coolant fluid can be modeled as single-phase, with the exception of freezing at very low temperatures, well outside of the operating range.

The coolant inlet at the base of the reactor cavity and along channels in the cylindrical central reflector guarantees that the salt flows upward and radially outward through the core.

1.b.3 Graphite Reflector Components

The reactor core is a cylindrical annulus around a central graphite reflector and surrounded on the outer boundary by an outer graphite reflector block. To protect the outer graphite reflector, the outer core region contains a layer of graphite pebbles. These components serve to moderate and reflect the neutrons within the core.

1.c Relevant Design Specifications

Additional design features specifically relevant to transient behavior include buoyantly driven control rods and blades, air heat exchangers, and an emergency natural circulation loop.

1.d Timescales of Salt and Pebble Movement

Since the salt coolant provides a strong negative feedback contribution, the timescale on which the heated salt moves out of the core is important. If the hot salt is replaced too quickly by cooled salt, then much of the negative temperature feedback from he coolant, contributing to safe shutdown, is lost.

Salt displacement, therefore, must be captured in any ATWS model of the PB-FHR core.

2 Review

Transient analysis is necessary when the neutron flux varies with time. Commonly studied transient scenarios include normal startup and shutdown of a reactor as well as abnormal scenarios that cause reactivity increases and decreases during otherwise normal operation.

Fundamentally, transient analyses seek to characterize the relationship between neutron population and temperature, which are coupled together by reactivity. That is, any change in power of a reactor can be related to a quantity known as the reactivity, ρ, which characterizes the offset of the nuclear reactor from criticality. In all power reactors, the the scalar flux of neutrons is what determines the reactor's power. The reactor power, in turn, affects the temperature. Reactivity feedback then results, due the temperature dependence of geometry, material densities, the neutron spectrum, and microscopic cross sections [4].

Nuclear reactors operate in state of criticality, which implies a steady state neutron flux (and hence power). Should the reactor deviate from criticality, a power transient will result. The magnitude and duration of the power transient will be dependent upon the length and strength of the deviation. In an ATWS, only intrinsic negative feedback responses within a reactor design are relied upon to prevent an uncontrollable power excursion. Since some feedback may be positive while other feedback is negative, an analysis of the balance must be addressed. Additionally, due to the effect of delayed neutrons, the timescales of fluid flow, heat conduction, thermal transport, or other phenomena, both positive and negative feedback may be delayed. Thus, a transient assessment of the time evolution of the neutron population within the core is essential to capture power-level instabilities resulting when reactivity feedback that is out-of-phase with the neutron population [5].

By combining the neutron transport equation with a source contribution from delayed neutrons, we arrive at the fundamental analysis tool in nuclear reactor kinetics. These are a stiff set of PDEs involving nonlinearly coupled neutronics, thermodynamics, and hydraulics.

The delayed neutron precursors obey the equation,

$$\frac{\partial \hat{C}_i(t,r)}{\partial t} = \beta_i \nu \Sigma_f(r,t)\phi(r,t) - \lambda_i \hat{C}_i(r,t) \tag{17}$$

where

$$i \in [1,6]. \tag{18}$$

β_i and λ_i depend on the incident neutron energy, fissionable isotope, and precursor group. In this way, the linearized Boltzmann transport equation has seven dimensions. Taking delayed neutrons into account, the one speed neutron diffusion equation can be written,

$$\frac{1}{v}\frac{\partial \phi(r,t)}{\partial t} - D(r,t)\nabla^2\phi(r,t) + \ \Sigma_a(r,t)\phi(r,t) = (1-\beta)\nu\Sigma_F(r,t)\phi(r,t) + \ \sum_{i=1}^{6} \lambda_i \hat{C}_i(r,t). \tag{19}$$

Transient analysis methods seek to solve this equation for changes in the parameters caused by a changing reactor conditions. Additional PDEs are added to this calculation to capture the dependence of temperature on heat conduction and the effect of fluid flow.

Fundamentally, there are two classes of method for solving this set of PDEs for neutron transport calculations. Deterministic methods solve the Boltzmann transport equation using a numerical approximation while stochastic methods model the system and solve the model statistically. Approaches for involving time dependence include 'operator splitting' as well as more tightly coupled methods and fully coupled methods such as the Jacobian-Free Newton Krylov (JFNK) approach.

2.a The Point Reactor Kinetics Equations

One common method to evaluate transient scenarios is through reduction of dimensions by the use of of the Point Reactor Kinetics Equations. If we assume a separation of variables solution to (19), we arrive at:

$$\phi(r,t) = vn(t)\psi_1(r) \tag{20}$$

$$\hat{C}_i(r,t) = C_i(t)\psi_1(r) \tag{21}$$

where ψ_1 is the fundamental mode solution of

$$\nabla^2\psi_n + B_g^2\psi_n = 0. \tag{22}$$

Using this separation of variables solution reduces the spatial complexity of the reactor to a single point. Inserting (20) and (21) into (19) gives the Point Reactor Kinetics Equations.

$$\begin{aligned} \frac{dn(t)}{dt} &= \frac{\rho(t)-\beta}{\Lambda}n(t) + \sum_{i=1}^{6}\lambda_i C_i(t) \\ \frac{dC_i(t)}{dt} &= \frac{\beta_i}{\Lambda}n(t) - \lambda_i C_i(t) \end{aligned} \tag{23}$$

where

$$\begin{aligned} i &\in [1,6] \\ \Lambda &\equiv (v\nu\Sigma_F)^{-1} \\ \rho(t) &\equiv \frac{k(t)-1}{k(t)} \\ &\equiv \frac{\nu\Sigma_F - \Sigma_a(1+L^2B_g^2)}{\nu\Sigma_F} \end{aligned}$$

and

$$k \equiv \frac{\nu\Sigma_F/\Sigma_a}{1+L^2B_g^2}.$$

The Point Reactor Kinetics Equationss (PRKEs) allow a nuclear engineer to remove the spatial aspects of the reactor from consideration, thereby only concerning themselves with the integral flux transients, which manifest as power transients. In addition to modeling the neutronic properties of a nuclear reactor, the PRKE can be modified to include the thermal-hydraulic feedback effects that the power transient will induce.

The PRKE are a set of stiff, nonlinear ordinary differential equations. For a reactor in which the only reactivity feedback comes from the fuel and the coolant:

$$\frac{d}{dt}\begin{bmatrix} p \\ \zeta_1 \\ . \\ . \\ . \\ \zeta_j \\ . \\ . \\ . \\ \zeta_J \\ \omega_1 \\ . \\ . \\ . \\ \omega_k \\ . \\ . \\ . \\ \omega_K \\ T_{fuel} \\ T_{cool} \\ T_{refl} \\ T_{matr} \\ T_{grph} \\ . \\ . \\ . \end{bmatrix} = \begin{bmatrix} \frac{\rho(t,T^{fuel},T_{cool},\cdots)-\beta}{\Lambda}p + \sum_{j=1}^{j=J}\lambda_j\zeta_j \\ \frac{\beta_1}{\Lambda}p - \lambda_1\zeta_1 \\ . \\ . \\ . \\ \frac{\beta_j}{\Lambda}p - \lambda_j\zeta_j \\ . \\ . \\ . \\ \frac{\beta_J}{\Lambda}p - \lambda_J\zeta_J \\ \kappa_1 p - \lambda_1\omega_1 \\ . \\ . \\ . \\ \kappa_k p - \lambda_k\omega_k \\ . \\ . \\ . \\ \kappa_{kp} - \lambda_k\omega_k \\ f_{fuel}(p, C_p^{fuel}, T_{fuel}, T_{cool}, \cdots) \\ f_{cool}(C_p^{cool}, T_{fuel}, T_{cool}, \cdots) \\ f_{refl}(C_p^{refl}, T_{fuel}, T_{refl}, \cdots) \\ f_{matr}(C_p^{matr}, T_{fuel}, T_{matr}, \cdots) \\ f_{grph}(C_p^{grph}, T_{fuel}, T_{grph}, \cdots) \\ . \\ . \\ . \end{bmatrix} \tag{24}$$

Equation 29, shows a generalized set of PRKE where variables include the normalized power, p, the delayed neutron precursor concentrations ζ_j, decay heats, ω_k, and the core average fuel and coolant temperatures T_{fuel} and T_{cool}. Additional equations quantifying other phenomena can add complexity to this suite of PDEs.

2.b Operator Splitting

Problems involving coupled physics are often solved with operator splitting techniques. In practice, this is typically in order to take advantage of separate physics codes that have been vetted and tested to efficiently solve the different physical aspects of the problem. Methods appropriate for the short time-scale diffusion of neutrons, for example, would be inappropriate for modeling the longer time scales of thermodynamic diffusion. Nonlinear coupling of the physical phenomena involved in the PRKE introduces the complication in which the solution is not as easily split into physically separate operators. When the separate physics are solved at a time step, it is not necessarily possible to calculate the nonlinear 'residuals' at the same time step. In this way, errors can be introduced into the nonlinearly coupled neutronics, hydraulics, and heat transfer physics of the PRKE.

Neutronics is primarily concerned with neutron populations. The production and destruction of neutrons in a reactor is dependent on reaction cross cross-sections. These characterize reaction probabilities and are dependent on material properties such as atomic density and temperature in both the moderator and the fuel.

Hydraulics is the study of the motion, density, and temperature of liquids. The liquid of interest in reactor physics is typically the moderator or coolant. The hydraulic properties of this liquid depend on the

characteristics of the cooling system, the heat transfer between the fuel and the moderator, etc.

Heat Transfer focuses on the heat generation in the reactor fuel and the removal of that heat by the moderator. Heat transfer behavior depends on everything from the moderator density and temperature to the neutron-driven power production in the fuel.

Thermal-Hydraulics is the area of this system that contains the majority of the nonlinearities. This is due to the polynomial forms that often arise in temperature dependencies of the material properties such as the heat capacity, density, and thermal conductivity for many coolant and fuel materials. The heat transfer coefficients can also be non-linear functions of several material properties.

The PRKE can be split clearly into a neutronics sub-block and a thermal-hydraulics sub-block which can be solved independently at each time step, combined, and solved again for the next time step. The two sub blocks are related by the reactivity term $\rho(t, T_{fuel}, T_{cool})$ in the first equation which depends on the fuel and coolant temperatures T_{fuel} and T_{cool}. The rest of the equations in the neutronics block are indirectly dependent on the reactivity via direct dependence on the power p. The neutronics sub-block consists of the first J+K+1 equations from Equation 29 :

$$\frac{d}{dt}\begin{bmatrix} p \\ \zeta_1 \\ . \\ . \\ . \\ \zeta_J \\ \omega_1 \\ . \\ . \\ . \\ \omega_K \end{bmatrix} = \begin{bmatrix} \frac{\rho(t,T_{fuel},T_{cool},\cdots)-\beta}{\Lambda}p + \sum_{j=1}^{j=J}\lambda_j\zeta_j \\ \frac{\beta_1}{\Lambda}p - \lambda_1\zeta_1 \\ . \\ . \\ . \\ \frac{\beta_J}{\Lambda}p - \lambda_J\zeta_J \\ \kappa_1 p - \lambda_1\omega_1 \\ . \\ . \\ . \\ \kappa_k p - \lambda_k\omega_k \end{bmatrix} \tag{25}$$

and the thermal-hydraulic sub-block consists of the equations describing the temperature dependence:

$$\frac{d}{dt}\begin{bmatrix} T_{fuel} \\ T_{cool} \\ . \\ . \\ . \end{bmatrix} = \begin{bmatrix} f(p, C_p^{fuel}, T_{fuel}, T_{cool}, \cdots) \\ g(C_p^{cool}, T_{fuel}, T_{cool}, \cdots) \\ . \\ . \\ . \end{bmatrix} \tag{26}$$

2.c The Jacobian

In order to avoid error introduced in the linear treatment of nonlinear terms, a Jacobian iteration or a Jacobian-Free Newton Krylov method can be used to solve the 'mono-block' of equations. These approaches approach solves the two types of physics together, with no lagging of the time steps. For the Jacobian approach, the explicit evaluation of the Jacobian is necessary, but for our stiff PDE application can be daunting.

For the 0D situation, that is, a situation in which we truly treat the reactor as a point, the finite set of equations involved could feasibly be solved using a regular, Jacobian-type Newton method. The only drawback to this is that in order to solve the triangular system at each time step, the Jacobian of the equation must be calculated.

The PRKEs in the above section is a $(3 + J + K)$ equation system of the form $dy/dt = F(y, t)$. It will therefore have a $(3 + J + K) \times (3 + J + K)$ Jacobian in which each term is a partial derivative such that $J_{ij}(y) = \frac{\partial}{\partial y_j}F_i(y)$. The calculation of such a thing is no small effort in Mathematica and would be disastrously time consuming by hand. A very small snippet of the Jacobian for that system follows.

$$J[F(y,t)] = \begin{bmatrix} \frac{\partial}{\partial p}\left(\frac{\rho(t,T_{eff}^{fuel},T_{cool})-\beta}{\Lambda}p + \sum_{j=1}^{j=J}\lambda_j\zeta_j\right) & \frac{\partial}{\partial p}\left(\frac{\beta_1}{\Lambda}p - \lambda_1\zeta_1\right) & \frac{\partial}{\partial p}\left(\frac{\beta_2}{\Lambda}p - \lambda_2\zeta_2\right) & . & . & . \\ . & . & . & & & \\ . & . & . & & & \\ . & . & . & & & \end{bmatrix} \quad (27)$$

In order to solve the non-linear system, a traditional newton method or other iteration scheme can be used. In such a method, Equation 28 is used iteratively to obtain the correct solution to the non-linear system. For newton, that is

$$y^{k+1} = y^k + J(y^k,t)^{-1}\,F(y^k,t). \quad (28)$$

2.d Jacobian Free Newton Krylov

Jacobian-Free Newton Krylov, however, does not require the explicit evaluation of the Jacobian in order to proceed toward the solution. Rather, it utilizes an iterative method called GMRES. It and other Krylov subspace methods eliminate the need for explicit formulation of that Jacobian matrix. These methods rely instead on the residual, that is, the *action* of the matrix on the solution. The only significant disadvantage to this method is the increased need for computational memory if a sufficiently accurate physics-based preconditioner is not used for accelerating the method.

In particular, the JFNK solution method [6], combined with physics-based preconditioning, enables extraordinary parallel scalability and fully-coupled solutions to systems of neutron transport and thermal hydraulic equations. Multiphysics Object-Oriented Simulation Environment (MOOSE), from INL, which relies on this exceptional numerical method as well as adaptive mesh refinement for structured and unstructured meshes, is beginning to be used in earnest for nuclear engineering applications (e.g., [7, 8, 9, 10, 11] among others). Moreover, the MOOSE tool possesses a modular, object-oriented simulation environment approach, which allows user-developers to construct applications by focusing on the unique physics of their modeling problem with minimal concern for the system solution methodology.

2.d.1 Conjugate Gradient Method

Another Krylov subspace method is the Conjugate Gradient Method. One extension to CG for non-symmetric systems is the Bi-Conjugate Gradient Stabilized (BiCGSTAB). BiCGSTAB is used in the Purdue Advanced Reactor Core Simulator (PARCS) software.

3 Previous Work

3.a Fratoni design work

In [12] and [13], assessments of reactivity coefficients for the Pebble Bed Advanced High Temperature Reactor (PB-AHTR) were made. Additionally, the Fratoni analysis showed that increased heavy metal loading in the pebbles both increased the Doppler resonance absorption (making the fuel temperature coefficient more negative) and allowed the coolant temperature feedback coefficient to be negative [13].

3.b Griveau PB-AHTR Transient Analysis

A RELAP5-3D analysis was conducted concerning the PB-AHTR. That analysis relied on an Monte Carlo N-Particle code (MCNP) model. The pebble fuel characteristics of both an annular and a homogeneous pebble design were analyzed. MCNP was used to analyze the reactivity variation of the pebble bed due to temperature changes. In this reactivity analysis, the effects of both Doppler broadening and material density were addressed. In RELAP5-3D in 2005-2006, material properties of salts including flibe were introduced [14].

Studies of LOFC transients within a similar reactor design, the Advanced High Temperature Reactor (AHTR), were conducted with the Graphite Reactor Severe Accident Code (GRSAC) tool. That tool is primarily a thermal hydraulics tool, but includes the ability to include point kinetics neutronics with xenon and samarium poisoning, in order to study ATWS [15].

Another type of event that is more challenging for the Fluoride-Salt-Cooled High-Temperature Reactor (FHR) is a LOHS in which the heat removal is interrupted, but the primary pumps continue to function. The fission power is then expected to be transferred from the core to the primary loop structures. This situation was investigated from a thermal hydraulics perspective by Blandford and Peterson [16] and relied on neutronic properties obtained from steady state calculations [12].

3.c Preliminary ATWS Analysis in the PB-FHR

Based on past analysis of the PB-AHTR [17, 13], the PB-FHR is expected to coast toward a safe shutdown in an unprotected LOFC event by relying primarily on natural circulation and the strongly negative prompt temperature reactivity feedback coefficient of the fuel. Additionally, the negative temperature reactivity feedback coefficients of the fuel and coolant drive the expectation that the PB-FHR will also survive LOHS and RIA events without damage to components. Temperature reactivity feedback coefficients in the PB-FHR, reported in [18] and are listed in Table 1.

PB-FHR Mk1 Reactivity Coefficients (Temperature)

Component	**Temperature Reactivity Coefficient** $[\frac{pcm}{K}]$
Fuel	-3.8
Coolant	-1.8
Inner Graphite Reflector	$+0.9$
Graphite Moderator	-0.7
Outer Graphite Reflector	$+0.9$

Table 1: PB-FHR Mk1 temperature coefficients of reactivity[18].

A detailed analysis of this behavior in each event scenario has not been conducted. However, a scoping study has implemented a loose coupling between the COMSOL Multiphysics solver and MCNP5, based on [17]. This scoping study has shown that under natural circulation alone, the maximum coolant temperature at the core outlet remains below 750°C in a LOFC ATWS.

In addition to this preliminary analysis focusing on the FHR core behavior, RELAP5 and Flownex models of the entire FHR system are being developed, based on older models of the PB-AHTR [19, 20]. These models include the whole FHR primary loop, DRACS loops, and coupling to the power conversion system through the CTAHs. They will initially be used during the FHR design phase to demonstrate performance and response to Licensing Basis Events (LBEs), but they can also be used to analyze FHR response to BDBEs, and ATWS in particular. Key performance criteria that can be tested using such models will include:

Maximum fuel and coolant temperatures, based on feedback between the core and the rest of the FHR subsystems; Time to achieve steady-state conditions in the FHR system after BDBEs; Changes to system response, should one or several DRACS loops fail, one or several main salt pumps trip, components of the power conversion system fail, etc.

Additonally, a PRKE analysis was conducted (by E. Greenspan [21]) which resulted in only moderate temperature increase for a RIA. Specifically, a prompt reactivity insertion of two dollars of reactivity resulted in a maximum fuel temperature of only approximately 1100°C.

4 Proposed Work

Work in this topic will occur in three main thrusts. The first thrust was to update previous work on transient analysis to accurately represent the Mark 1 core. This current phase requires adjustments to current MCNP5 and COMSOL model geometries as well as incorporation of graphite reactivity data into the neutronics analysis. This phase will enable replication of previous steady state assessments of beginning

and end of transient core states. Additionally, it will include scoping studies to discern the need for coupling tightness in the next phases.

The second phase will implement a deterministic transient neutronics model in a platform suited to loose temporal and spatial coupling between the neutronics and thermal hydraulics. This will rely on data from current MCNP, Reactor Excursion and Leak Analysis Program (RELAP) and COMSOL models.

The third phase will emphasize high fidelity coupled multiphysics. Work from the second phase will be imported into a high performance multiphysics environment, MOOSE, which enables tight coupling between a large ecosystem of physical models and solvers. In particular MOOSE will enable tight RELAP7 thermal hydraulics coupling with deterministic neutronics solvers. Once this step is complete, additional physics analyses can be easily added to the model in a tightly coupled fashion using the ecosystem of tools available in MOOSE. These include tools capable of modeling multiscale fuel performance analysis, long term component material degradation modeling, and mass and energy transport in coolants.

4.a Phase I : Scoping Study

In 2012, Pod, a transient thermal hydraulics model in COMSOL, was created for the large PB-AHTR core design [17]. It has been modified to represent the Mark 1 PB-FHR core design. Simultaneously, current neutronics efforts relying on probabilistic methods were updated (by Cisneros in [18]). These MCNP results were then coupled to Pod for scoping studies of the Mk1.

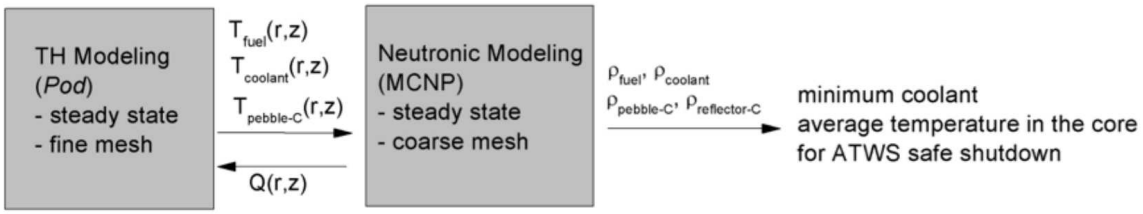

Figure 2: Current work has been limited to loose coupling between two steady state models.

A detailed analysis of this behavior in each event scenario has not been conducted. However, a scoping study has implemented a loose coupling between the COMSOL Multiphysics solver and MCNP5, based on the COMSOL model designed for the PB-AHTR [17]. This scoping study has shown that under natural circulation alone, the maximum coolant temperature at the core outlet remains below 750°C in a LOFC ATWS. Those results can be seen in Figure 4.

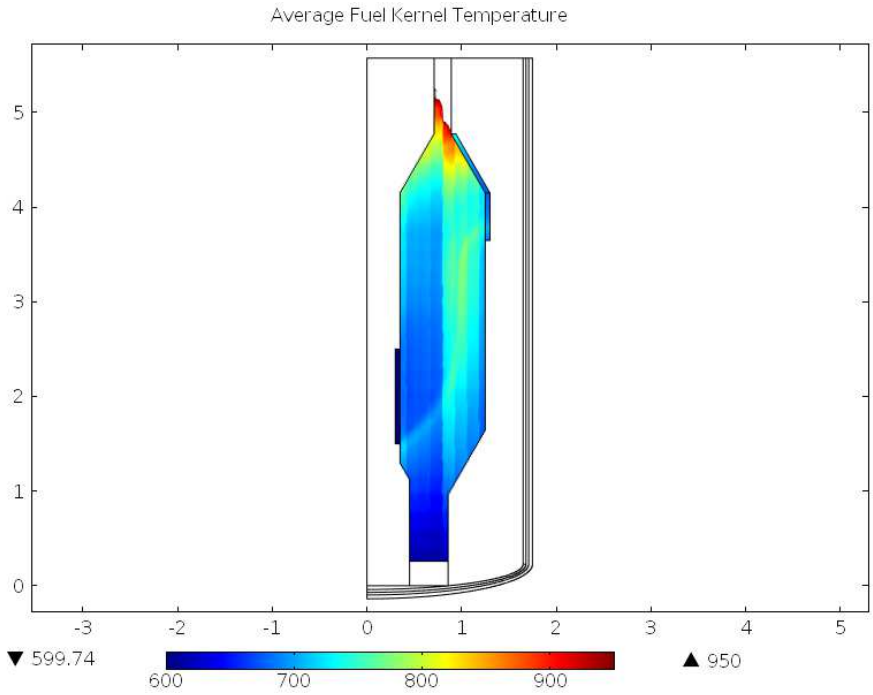

Figure 3: A scoping study in COMSOL demonstrates the steady state temperature profile of the fuel in the core in the event of natural circulation alone.

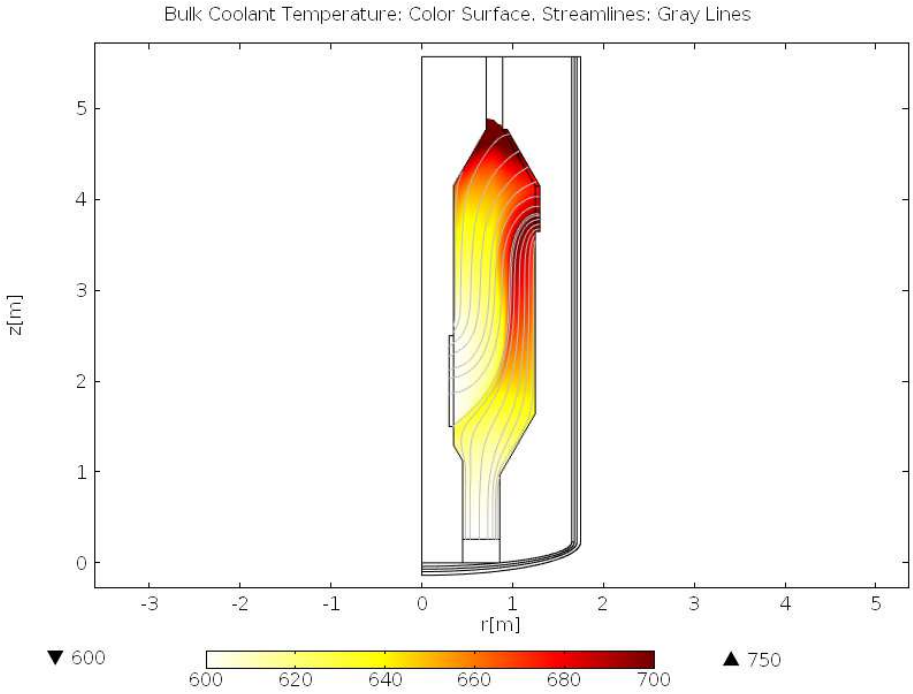

Figure 4: A scoping study in COMSOL demonstrates the steady state temperature profile of the coolant in the core in the event of natural circulation alone.

4.b Phase II : Zero Dimensional Coupled Transient Model

A scoping study will arrive at a first order approximations of transient behavior based on 0-D coupled neutron kinetics and thermal hydraulics in the Mark 1 PB-FHR. This scoping study will include parameterized analysis of LOFC, LOHS, LOLA, and RIA scenarios of varying severity and duration. It will also address various coupling strategies to measure the sensitivity of the analysis to coupling tightness.

A point reactor kinetics analysis of the PB-FHR will utilize results from previous MCNP analyses of the Mark 1 design [18] as well as thermal hydraulics estimations for that design. The following is the driving set of partial differential equations:

$$\frac{d}{dt}\begin{bmatrix} p \\ \zeta_1 \\ . \\ . \\ . \\ \zeta_j \\ . \\ . \\ . \\ \zeta_J \\ \omega_1 \\ . \\ . \\ . \\ \omega_k \\ . \\ . \\ . \\ \omega_K \\ T_{fuel} \\ T_{cool} \\ T_{refl} \\ T_{matr} \\ T_{grph} \\ . \\ . \\ . \end{bmatrix} = \begin{bmatrix} \frac{\rho(t,T^{fuel},T_{cool},\cdots)-\beta}{\Lambda}p + \sum_{j=1}^{j=J}\lambda_j\zeta_j \\ \frac{\beta_1}{\Lambda}p - \lambda_1\zeta_1 \\ . \\ . \\ . \\ \frac{\beta_j}{\Lambda}p - \lambda_j\zeta_j \\ . \\ . \\ . \\ \frac{\beta_J}{\Lambda}p - \lambda_J\zeta_J \\ \kappa_1 p - \lambda_1\omega_1 \\ . \\ . \\ . \\ \kappa_k p - \lambda_k\omega_k \\ . \\ . \\ . \\ \kappa_{kp} - \lambda_k\omega_k \\ f_{fuel}(p, C_p^{fuel}, T_{fuel}, T_{cool}, \cdots) \\ f_{cool}(C_p^{cool}, T_{fuel}, T_{cool}, \cdots) \\ f_{refl}(C_p^{refl}, T_{fuel}, T_{refl}, \cdots) \\ f_{matr}(C_p^{matr}, T_{fuel}, T_{matr}, \cdots) \\ f_{grph}(C_p^{grph}, T_{fuel}, T_{grph}, \cdots) \\ . \\ . \\ . \end{bmatrix} \tag{29}$$

Written in Python, the pbfhr/prke software is able to utilize python modules within the PyNE toolkit.

4.b.1 Coupling

In this implementation, the Forward Euler coupling method is used. Here, we treat neutronics and thermal hydraulics separately at each time step with **forward Euler**. The values for T_f, T_c, T_m, and T_r at time t_n are passed between physics subblocks, and the process is repeated according to the following scheme:

$$U^n = \begin{bmatrix} N^n \\ T^n \end{bmatrix} \tag{30}$$

$$N^{n+1} = N^n + kf(U^n) \tag{31}$$

$$U^* = \begin{bmatrix} N^{n+1} \\ T^n \end{bmatrix} \tag{32}$$

$$T^{n+1} = T^n + kf(U^*) \tag{33}$$

4.b.2 Neutronics Data Needs

The data needs in the neutronics block include the following variables:

$$\rho(t,T_f,T_c,T_m,T_r) = \text{ reactivity, [pcm]} \tag{34}$$

$$\beta = \text{ fraction of neutrons that are delayed} \tag{35}$$

$$\beta_j = \text{ fraction of delayed neutrons from precursor group j} \tag{36}$$

$$\zeta_j = \text{ concentration of precursors of group j} \tag{37}$$

$$\lambda_j^d = \text{ decay constant of precursor group j} \tag{38}$$

$$\Lambda = \text{ mean generation time ?} \tag{39}$$

$$\omega_k = \text{ decay heat from FP group k} \tag{40}$$

$$\kappa_k = \text{ heat per fission for decay FP group k} \tag{41}$$

$$\lambda_k^{FP} = \text{ decay constant for decay FP group k} \tag{42}$$

To satisfy these data needs, standards for fission in U235 were used along with the reactivity coefficient results in Table 1.

For the 6-group delayed neutron precursors, the data in Table 2 was used.

j	$t_{1/2}$ $[s]$	λ_j^d $[1/s]$	η_j $[n/f]$	β_j
1	55.72	0.0124	0.00052	0.000215
2	22.72	0.0305	0.00546	0.001424
3	6.22	0.111	0.00310	0.001274
4	2.30	0.301	0.00624	0.002568
5	0.614	1.14	0.00182	0.000748
6	0.230	3.01	0.00066	0.000273

Table 2: Delayed neutron data, ^{235}U thermal fission [22].

For the 11-group decay heat model, the data in Table 3 was used.

k	λ^{FP_k} $[1/s]$	κ_k $[MeV/fission-s]$
1	6.587×10^{0}	2.658×10^{0}
2	1.490×10^{-1}	4.619×10^{-1}
3	2.730×10^{-1}	6.069×10^{-2}
4	2.173×10^{-2}	5.593×10^{-3}
5	1.961×10^{-3}	6.872×10^{-4}
6	1.025×10^{-4}	6.734×10^{-5}
7	4.923×10^{-6}	6.413×10^{-6}
8	2.679×10^{-7}	6.155×10^{-7}
9	1.452×10^{-8}	8.288×10^{-8}
10	1.893×10^{-9}	1.923×10^{-8}
11	1.633×10^{-10}	1.214×10^{-9}

Table 3: Decay heat data, ANS/ANSI 5.1-1971 for ^{235}U thermal fission.

4.b.3 Thermal Hydraulics Data Needs

The thermal hydraulics behavior within the reactor core has previously been modeled within COMSOL using porous medium approximations. For the 0-D effort, the driving equations can be modeled with lumped capacitance, which approximates heat transfer into discrete components, approximating the effects of geometry.

Fundamentally, heat transfer through a system of components is modeled analogously to current through a resistive circuit. Table 4 describes the various canonical forms of lumped capacitance heat transfer modes.

Based on the modes in Table 4, we can formulate a model for the PB-FHR component temperatures in the low density graphite core of the pebble, the graphite matrix in the fuel annulus of the fuel pebble, the high density graphite pebble shell, the fuel (TRISO particles pebble fuel annulus), coolant, and reflectors. A diagram of the components is found in 5.

Fundamentally, to determine the temperature change in the body, we rely on relations between temperature, heat capacity, and thermal resistance. As in Table 4, the heat flow out of body i is the sum of surface heat flow by conduction, convection, radiaion, and other mechanisms to each adjacent body, j [24]:

$$Q = Q_i + \sum_j Q_{ij} \tag{43}$$

$$= Q_i + \sum_j \frac{T_i - T_j}{R_{th,ij}} \tag{44}$$

Transfer Mode	Rate of Heat Transfer	Thermal Resistance
Conduction	$\dot{Q} = \frac{T_1 - T_2}{\left(\frac{L}{kA}\right)}$	$\frac{L}{kA}$
Convection	$\dot{Q} = \frac{T_{surf} - T_{envr}}{\left(\frac{1}{h_{conv} A_{surf}}\right)}$	$\frac{1}{h_{conv} A_{surf}}$
Radiation	$\dot{Q} = \frac{T_{surf} - T_{surr}}{\left(\frac{1}{h_r A_{surf}}\right)}$	$\frac{1}{h_r A}$ $h_r = \epsilon\sigma(T_{surf}^2 + T_{surr}^2)(T_{surf} + T_{surr})$

Table 4: Lumped Capacitance for various heat transfer modes [23].

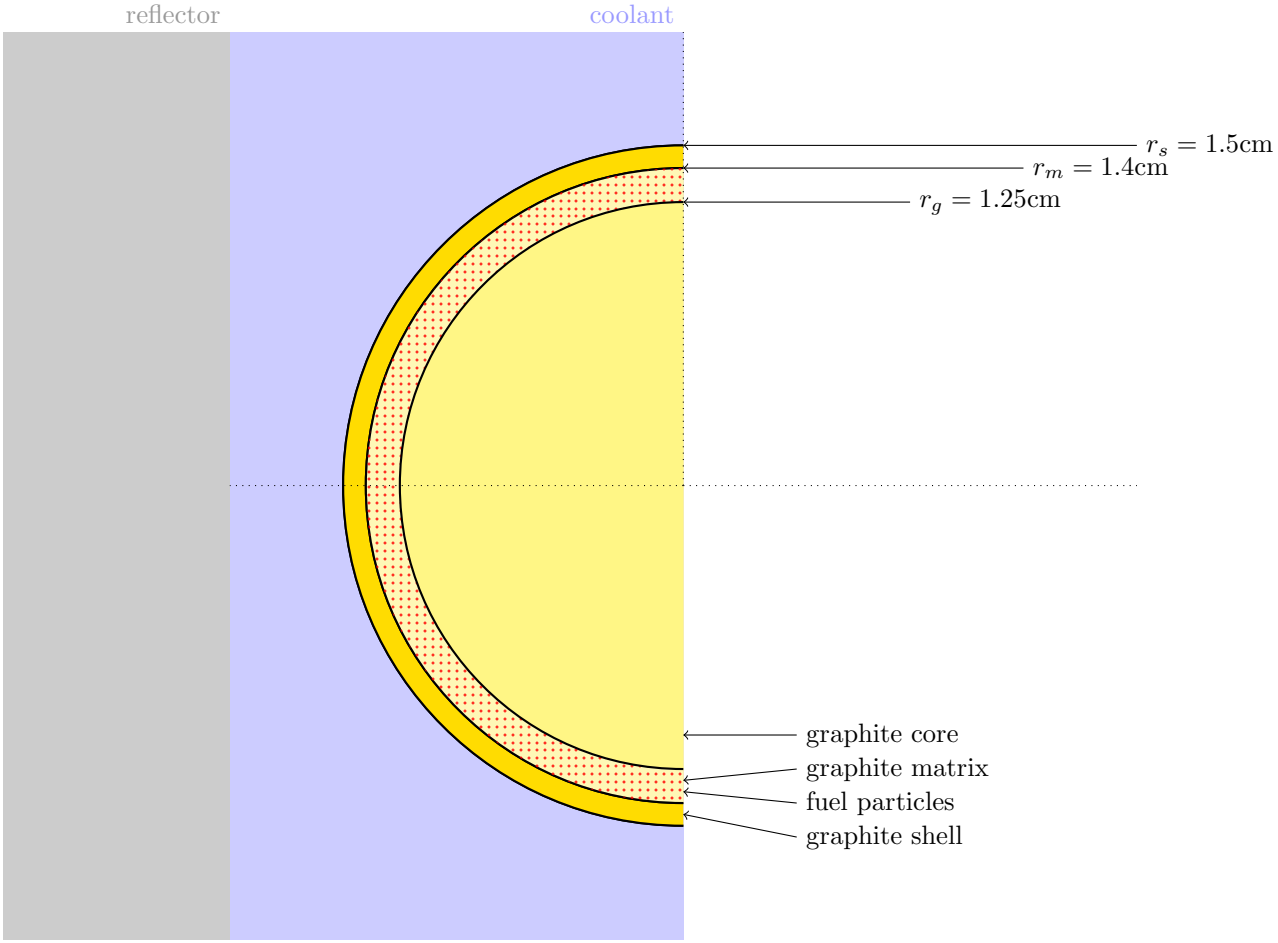

Figure 5: The components of the thermal system, from the TRISO fuel kernels to the reflector bodies, are shown conceptually here.

where

$$\dot{Q} = \text{total heat flow out of body i } [J \cdot s^{-1}] \tag{45}$$
$$Q_i = \text{other heat transfer, a constant } [J \cdot s^{-1}] \tag{46}$$
$$T_i = \text{temperature of body i } [K] \tag{47}$$
$$T_j = \text{temperature of body j } [K] \tag{48}$$
$$j = \text{adjacent bodies } [-] \tag{49}$$
$$R_{th} = \text{thermal resistence of the component } [K \cdot s \cdot J^{-1}]. \tag{50}$$

Note also that the thermal energy storage and release in the body is accordingly related to the heat flow via capacitance:

$$\frac{dT_i}{dt} = \frac{-Q + \dot{S}_i}{C_i} \tag{51}$$

where

$$C = \text{heat capacity of the object } [J \cdot K^{-1}] \tag{52}$$
$$= (\rho c_p V)_i \tag{53}$$
$$\dot{S}_i = \text{source term, thermal energy conversion } [J \cdot s^{-1}] \tag{54}$$

Together, these form the equation:

$$\frac{dT_i}{dt} = \frac{-\left[Q_i + \sum_j \frac{T_i - T_j}{R_{th,ij}}\right] + \dot{S}_i}{(\rho c_p V)_i} \tag{55}$$

Low Density Graphite Core Temperature The inner low density graphite at the core of the fuel pebble acts as a neutron moderator and heat sink. That physical component only interacts with the graphite in the fuel matrix layer. It acts as a heat sink for the fuel matrix layer.

There is no other heat transfer out of (so $Q_i = 0$) and no heat generation in the moderator (so $\dot{S}_i = 0$). The heat transfer between two solid components is conductive, so the thermal resistance between the moderator and fuel is of the form $R_{th} = L/kA$. Accordingly, the model for temperature in the moderator could then be described as :

$$\frac{dT_I}{dt} = -\frac{\left[\frac{T_I - T_M}{R_{th,IM}}\right]}{(\rho c_p V)_I} \tag{56}$$

In our case, the area, A, is the surface area of all N_p the internal, moderating, low-density graphite sphere, and the length constant is simply r_I, its radius, so

$$R_{th,IM} = \frac{r_I}{k_I A_{IM}} \tag{57}$$
$$= \frac{r_I}{4\pi N_p r_I^2 k_I} \tag{58}$$
$$= \frac{1}{4\pi N_p r_I k_I} \tag{59}$$

and, therefore,

$$\frac{dT_I}{dt} = -\frac{4\pi N_p r_I k_I \left[T_I - T_M\right]}{(\rho c_p V)_I}. \tag{60}$$

Additionally, the volume of the inner, low-density graphite core is known. It is the volume of N_p spheres of radius r_I:

$$V_I = \frac{4}{3}\pi N_p r_I^3 \tag{61}$$

Matrix Graphite Temperature The graphite between TRISO particles in the fuel matrix layer is an extension of the low density graphite in the core. It is a conductive heat sink for the fuel particles, but is a conductive heat source to the low density graphite core and the high density graphite shell. Combining the contributions from each of these components gives:

$$\frac{dT_M}{dt} = -\frac{\left[\frac{T_M - T_I}{R_{th,MI}}\right]}{(\rho c_p V)_M} \tag{62}$$

$$-\frac{\left[\frac{T_M - T_F}{R_{th,MF}}\right]}{(\rho c_p V)_M} \tag{63}$$

$$-\frac{\left[\frac{T_M - T_S}{R_{th,MS}}\right]}{(\rho c_p V)_M} \tag{64}$$

$$\tag{65}$$

Since the length scale is the width of the annulus, $r_M - r_I$, the thermal resistence terms are:

$$R_{th,MI} = \frac{r_M - r_I}{k_M A_{MI}} \tag{66}$$

$$= \frac{r_M - r_I}{4k_M N_p \pi r_I^2} \tag{67}$$

$$R_{th,MF} = \frac{r_M - r_I}{k_M A_{MF}} \tag{68}$$

$$= \frac{r_M - r_I}{k_M N_p N_T 4\pi r_T^2} \tag{69}$$

$$R_{th,MS} = \frac{r_M - r_I}{k_M A_{MS}} \tag{70}$$

$$= \frac{r_M - r_I}{4k_M N_p \pi r_M^2} \tag{71}$$

where

$$N_T = \text{number of TRISO particles per pebble} \tag{72}$$

$$r_T = \text{radius a TRISO particle} \tag{73}$$

and, therefore,

$$\frac{dT_M}{dt} = -\frac{4k_M \pi N_p r_I^2 \left[T_M - T_I\right]}{\left(r_M - r_I\right)\left(\rho c_p V\right)_I} \tag{74}$$

$$= -\frac{4k_M \pi N_p N_T r_T^2 \left[T_M - T_I\right]}{\left(r_M - r_I\right)\left(\rho c_p V\right)_I} \tag{75}$$

$$= -\frac{4k_M \pi N_p r_M^2 \left[T_M - T_I\right]}{\left(r_M - r_I\right)\left(\rho c_p V\right)_I}. \tag{76}$$

Additionally, the volume of the matrix graphite is the volume of N_p spheres of radius r_M minus V_I and minus $N_p N_T$ spheres of radius r_T:

$$V_M = \frac{4}{3}\pi \left[N_p r_M^3 - N_p r_I^3 - N_p N_T r_T^3 \right]. \tag{77}$$

Shell Graphite Temperature The high density graphite shell is a thin layer between the matrix graphite and the coolant. The shell is adjacent to the matrix graphite component on its inner boundary and adjacent to the coolant on its outer boundary. These two components contribute to the temperature change:

$$\frac{dT_S}{dt} = \frac{-\left[\frac{T_S - T_M}{R_{th,SM}} + \frac{T_S - T_C}{R_{th,SC}}\right]}{(\rho c_p V)_S}. \tag{78}$$

At the inner boundary, heat transfer is conductive. However, at the outer boundary, it is convective, and the convective surface area between the pebble shells and the coolant is the set of N_p shells of radius r_S. Thus,

$$R_{th,SM} = \frac{r_S - r_M}{k_f A_{fm}} \tag{79}$$

$$= \frac{r_f}{4\pi N_p r_m^2 k_f} \tag{80}$$

$$= \frac{1}{4\pi N_p r_m k_f} \tag{81}$$

$$R_{th,SC} = \frac{1}{h_S A_{SC}} \tag{82}$$

$$= \frac{1}{4\pi N_p r_S^2 h_S} \tag{83}$$

$$V_S = \frac{4}{3}\pi N_p (r_S^3 - r_M^3) \tag{84}$$

Fuel Temperature Thousands of TRISO fuel particles generate fission power in the annulus surrounding the low-density graphite core of each pebble. These transfer heat to the graphite in the annulus. The fuel matrix component therefore only interacts with the matrix graphite component.

As above, the heat transfer between two solid components is conductive. The source term $\dot{S}_f$ is nonzero in this case. Indeed, it is the fission power generation, p, in the fuel for the whole pebble bed. Therefore, (55) in this case becomes

$$\frac{dT_F}{dt} = \frac{-\left[\frac{T_F - T_M}{R_{th,FM}} + \frac{T_F - T_S}{R_{th,FS}}\right] + p}{(\rho c_p V)_F}. \tag{85}$$

Here, the surface area between the matrix graphite and the fuel is the set of $N_p N_T$ shells of radius r_T. Additionally, the volume is the sum of $N_P N_T$ spherical volumes of radius r_T.

$$R_{th,FM} = \frac{r_F}{k_F A_{FM}} \tag{86}$$
$$= \frac{r_F}{4\pi N_p r_M^2 k_F} \tag{87}$$
$$= \frac{1}{4\pi N_p r_M k_F} \tag{88}$$
$$R_{th,FS} = \frac{r_F}{k_F A_{FS}} \tag{89}$$
$$= \frac{r_F}{4\pi N_p r_S^2 k_F} \tag{90}$$
$$= \frac{1}{4\pi N_p r_S k_F} \tag{91}$$
$$\tag{92}$$

Coolant Temperature The coolant is heated as it flows through the pebble bed and releases heat to the reflectors. Additionally, the pumping process moves hot (T_{out}) coolant out of the top of the core, to be replaced by cooler (T_{in}) coolant at the bottom of the core. The coolant temperature therefore varies in time and in space and an external mass-transfer heat flow, Q_c, must be accounted for in the coolant. Thus, (55) becomes:

$$\frac{dT_C}{dt} = \frac{-\left[Q_C + \frac{T_C - T_S}{R_{th,CS}} + \frac{T_C - T_r}{R_{th,CR}}\right]}{(\rho c_p V)_C} \tag{93}$$

That mass-transfer heat flow, Q_C can be defined in terms of $\dot{m}$, the mass flow rate, where T_{in} and T_{out} are the inlet and outlet coolant temperature in the reactor core:

$$Q_C = -\dot{m} c_{p,C} (T_{out} - T_{in}) \tag{94}$$

The convective heat transfer from the coolant to the pebble shells, $R_{th,CS}$, is the reverse of $R_{th,FS}$ defined above. Therefore,

$$R_{th,SC} = \frac{1}{h_S A_{CS}} \tag{95}$$
$$= \frac{1}{4\pi N_p r_S^2 h_S} \tag{96}$$
$$\tag{97}$$

Additionally, it releases some heat to the graphite central reflector and the outer reflector. In this formulation of the problem, all reflector bodies are taken to be a single component. The convective heat transfer between the coolant and reflectors is then:

$$R_{th,CR} = \frac{1}{h_R A_{CR}} \tag{98}$$

Reflector Temperature The inner and outer reflector are heated by the coolant in the core, but are simultaneously cooled by internal channels through which the cold inlet coolant flows. This complex thermal situation will be simplified in this model. The reflectors are taken to be a single body that dissipates heat to an environment at the coolant inlet temperature. The heat dissipated from the reflectors into that thermal sink can be estimated with an effective conduction coefficient, $k_{r,eff}$, so that (55) for this component becomes

$$\frac{dT_R}{dt} = \frac{-1}{\rho_R V_R c_{p,R}} \left[h_R A_R (T_C - T_R) - \frac{k_{R,eff} A_R}{L_{R,eff}} (T_R - T_{in}) \right]. \tag{99}$$

Data Needs Summary Parameters needed to fully define the above model include all of those listed in Table 5.

Mk1-PB-FHR TH Design Parameters

Symbol	Meaning	Value	Units	Source
N_p	Number of Pebbles	4.7×10^5	$[-]$	[25]
N_{rp}	Number of Reflector Pebbles	2.18×10^5	$[-]$	[25]
r_m	Moderator Radius	0.0125	$[m]$	[25]
r_f	Fuel Radius	0.014	$[m]$	[25]
r_s	Shell Radius	0.015	$[m]$	[25]
V_m	Moderator Volume	3.8451785083	$[m^3]$	[-]
V_f	Fuel Volume	1.55702044301	$[m^3]$	[-]
V_c	Coolant Volume	7.2	$[m^3]$	[25]
V_{or}	Outer Reflector Volume	24.89080459770115	$[m^3]$	[25]
V_{ir}	Inner Reflector Volume	3.413793103448276	$[m^3]$	[25]
V_{rp}	Reflector Pebble Volume	3.08190239317	$[m^3]$	[25]
A_{cr}	Reflector Surface Area	804.87603785	$[m^2]$	[-]
m_{or}	Outer Reflector Mass	4.3310×10^4	$[kg]$	[25]
m_{ir}	Inner Reflector Mass	5.940×10^3	$[kg]$	[25]
k_m	Moderator Thermal Conductivity	0.26 (for firebrick)	$[\frac{J}{s \cdot m \cdot K}]$	[25]
k_c	Coolant Thermal Conductivity	1.0	$[\frac{J}{s \cdot m \cdot K}]$	[26, 25]
k_f	Fuel Thermal Conductivity	$< +val+ >$	$[\frac{J}{s \cdot m \cdot K}]$	[?]
$k_{r,eff}$	Reflector Thermal Conductivity	0.26	$[\frac{J}{s \cdot m \cdot K}]$	[25]
ρ_m	Moderator Density	1.740×10^3	$[\frac{kg}{m^3}]$	[25]
ρ_f	Fuel Density	1.740×10^3	$[\frac{kg}{m^3}]$	[25]
ρ_f	Shell Density	1.767×10^3	$[\frac{kg}{m^3}]$	[25]
ρ_c	Coolant Density	$2330. - 0.42T$	$[\frac{kg}{m^3}]$	[26]
ρ_r	Reflector Density	1.740×10^3	$[\frac{kg}{m^3}]$	[25]
$c_{p,m}$	Moderator Specific Heat Capacity	684	$[\frac{J}{kg \cdot K}]$	[27]
$c_{p,f}$	Fuel Specific Heat Capacity	$< +val+ >$	$[\frac{J}{kg \cdot K}]$	[?]
$c_{p,c}$	Coolant Specific Heat Capacity	2380	$[\frac{J}{kg \cdot K}]$	[26]
$c_{p,r}$	Reflector Specific Heat Capacity	684	$[\frac{J}{kg \cdot K}]$	[27]
h_f	Pebble Bed Heat Transfer Coefficient	4700	$[\frac{J}{s \cdot m^2 \cdot K}]$	[25]
h_r	Reflector Heat Transfer Coefficient	$< +val+ >$	$[\frac{J}{s \cdot m^2 \cdot K}]$	[?]
$\dot{m}$	Coolant Mass Flow Rate	976	$[\frac{kg}{s}]$	[25]
T_{in}	Inlet Temperature	873.15	$[K]$	[25]
$L_{r,eff}$	Reflector Effective Length Constant	$< +val+ >$	$[m]$	[?]

Table 5: ¡+Caption text+¿

4.b.4 Heat transfer between solid phase and liquid phase in pebble bed

Using the Wakao correlation for the heat transfer coefficient, the fluid-to-pebble Nusselt number is

$$Nu = \frac{hL}{k} = 2 + 1.1 Pr^{1/3} Re^{0.6} \tag{100}$$

The Reynolds number and the Prandtl number are defined as follows:

$$\begin{aligned} Re &= \frac{\rho d_p U}{\mu} \\ d_p &= \text{diameter of a pebble} \\ U &= \frac{v_i}{\epsilon} \\ v_i &= \text{velocity at inlet} \\ \epsilon &= \text{porosity} \end{aligned}$$

and

$$Pr = \frac{c_p \mu}{k} \tag{101}$$

Properties such as μ, dynamic viscosity, k, thermal conductivity of FLiBe, are given as (temperature in C) :

$$\begin{aligned} \mu &= 4.638 * 10^5 (kg/m - s) \\ \rho &= 2279.92 - 0.488T (kg/m^3) \\ c_p &= 2415.78 (J/kg - K) \\ k &= 0.7662 + 0.0005T (W/m - K) \end{aligned} \tag{102}$$

The heat transfer coefficient h can then be calculated from the Nusselt number:

$$h = \frac{Nuk}{d_p}$$

where d_p is the pebble diameter, $0.03m$.

Thus,

$$h = \frac{(2 + 1.1 Pr^{1/3} Re^{0.6})(0.7662 + 0.0005T)}{0.03} \tag{103}$$

$$= \frac{\left[2 + 1.1 \left(\frac{2415.78 \times 4.638 \times 10^5}{0.7662 + 0.0005T}\right)^{1/3} \left(\frac{(2279.92 - 0.488T)(0.03)U}{4.638 \times 10^5}\right)^{0.6})(0.7662 + 0.0005T\right]}{0.03} \tag{104}$$

4.c Phase II: Application Prototype Development

To faithfully model accident transient response in the PB-FHR, a an application should be developed that is models fully-coupled, thermal-hydraulic and neutronic phenomena in three dimensions. This application should be benchmarked against other tools, in the absence of available experimental data for this design. Experimental benchmarking may be possible in collaboration with the team at SINAP building a prototype FHR.

The PRONGHORN[28] application has already been developed to serve this purpose for gas-cooled pebble-bed and prismatic fueled reactors. PRONGHORN is built for use within the sophisticated, open source, NQA-1 assured MOOSE framework. PRONGHORN results for a PBMR400 benchmark were well-matched to other codes [28], indicating promise for use of PRONGHORN for the PB-FHR. PRONGHORN has the ability to capture multi-dimensional thermal-fluid and neutronics transient problems implicitly in parallel.

4.c.1 Geometry

For PRONGHORN to be adapted to this purpose, mesh-generation for the PB-FHR Mk1 core is a key need. In particular, capturing the double heterogeneity of the PB-FHR fuel form is a specific challenge for this work.

Open source tools available for this include the MeshKit utility from Argonne National Laboratory (ANL), the MOAB library, and many others. Since MeshKit has been tested for exodus format mesh compatibility with PRONGHORN, it is a natural choice for generating a mesh to represent the geometric features of the PB-FHR. However, the Python toolkit for Nuclear Engineering (PyNE) toolkit has an interface to MOAB that is user friendly. With this interface, I have built a script for meshing annular fuel pebbles in a FLiBe volume

4.c.2 Materials

Additionally, an effort to define materials such as the FLiBe coolant in the PB-FHR is necessary in order to utilize the PRONGHORN tool for PB-FHR ATWS analysis. This will rely on standards for nuclear material definitions where possible. The mesh in Figure 6 was built with the PyNE tool and has attached material metadata indicating nodes that contain the FLiBe, fuel matrix, and graphite, respectively.

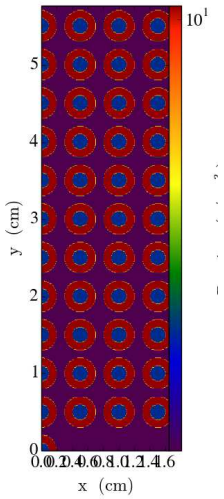

Figure 6: A 2D slice of a 3D mesh of annular fuel pebbles in a FLiBe fluid volume. The colors indicate the relative absorption cross sections. Created by a PyNE ipython notebook developed for this purpose : (http://nbviewer.ipython.org/github/katyhuff/pbfhr/blob/master/MeshPBFHR.ipynb)

4.c.3 Benchmarking Efforts

Benchmarking exercises should occur simultaneously, and indeed, should drive this prototype application development effort.

Initial benchmarking efforts should involve code-to-code confirmation of steady state, simple geometry, single-effect behavior. That is, a first benchmark comparison of the MOOSE-based application should compare the flux profile and eigenvalue calculation of a model as simple as a single fuel pebble sphere with reflective boundary conditions against the results from other codes. The effect of temperature, fuel composition, and geometry should each be varied independently so that single effects can be compared. As those benchmarks succeed, code validation exercises capturing multiple effects as well as more detailed core geometry can be pursued in turn.

Validation codes should include stochastic codes such as MCNP and Serpent, which are quick to prototype. The MCNP validation effort should utilize previous work by making exact comparisons to the current MCNP model of the Mk1 core. Additional models in Serpent can be developed alongside the MOOSE application. Additionally, a comparison to results from the deterministic, Krylov-subspace tool, PARCS, should be considered. Since development of a model in PARCS is likely to be as time-consuming as development of a MOOSE prototype, a collaboration should be pursued so that any PARCS comparison model is independently developed by a separate researcher.

4.d Phase III: High Fidelity Multiphysics

The final thrust of this work will be to perform an array of transient simulations, focusing on ATWS and RIA. A key feature of this thrust will be to conduct the appropriate analytical and computational validation work that will be neceessary to confirm confidence in the results of these transient simulations with the MOOSE application.

4.d.1 Calculation Requirements

A single transient simulation will need to calculate the reactor eigenvalue (k_{eff}) at a high time resolution over the course of at least a few seconds. Appropriate time resolution for a transient is on the order of a 0.01-0.001s. So, for a high fidelity simulation, the eigenvalue calculation will take place approximately once for every 0.001s simulated.

For a few-second transient, it will therefore need to be calculated on the order of 1000 times. The 3D simulation of a PB-FHR transient will have performance behavior that is similar to previous transient simulations run with PRONGHORN and MOOSE. Those simulations have been run already at INL [11, 28].

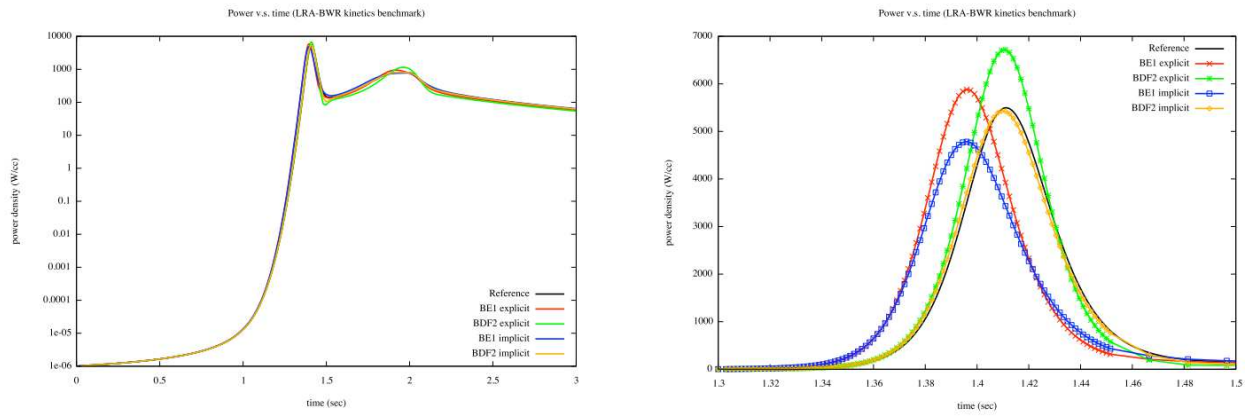

Figure 7: A similar multiphysics transient calculation using the PRONGHORN tool required on the order of 1500 eigenvalue calculations [11].

Figure 7 shows the results of a medium fidelity simulation over a few-second timespan using the PRONGHORN and MOOSE tools. Approximately 1500 eigenvalue calculations were required for this result (I will be using the BDF2 implicit calculation type that is yellow in the figure).

4.d.2 Expected Scaling Behavior

Performance scaling studies have been conducted with the PRONGHORN tool as well. In Figure 9 of Reference 1, the scaling behavior of a 2D eigenvalue problem is shown. That effort indicates, as in Figure 8 that for a single 2D eigenvalue calculation, 500 normalized hours of CPU time may be required for a relative error less than 10^{-3}.

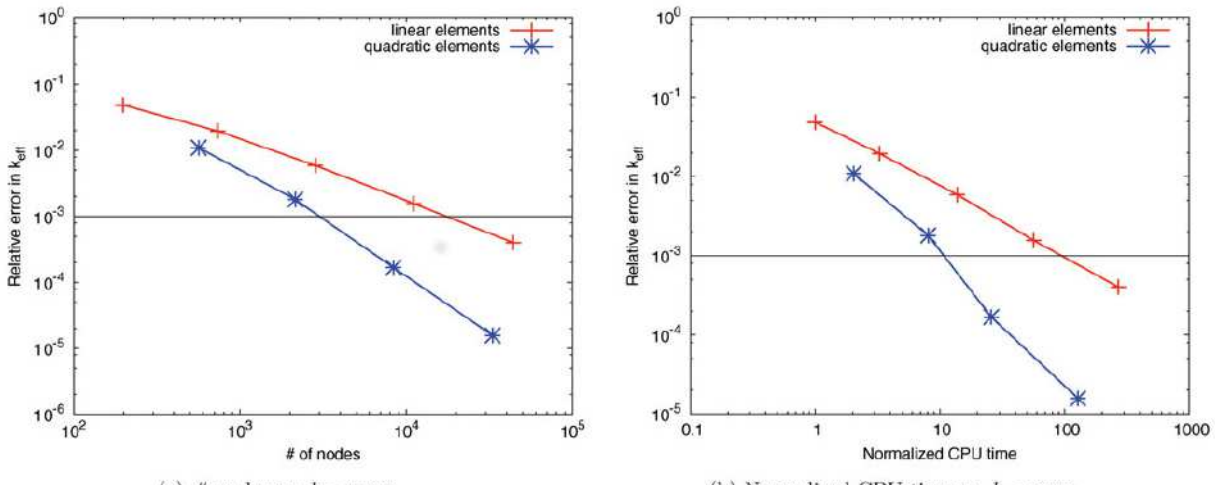

Figure 8: The CPU scaling behavior is nonlinear for a 2D transient simulation with PRONGHORN and MOOSE [28].

A 3D simulation will require more CPU time, but the factor of increase is unknown. Assuming a factor of two additional runtime for increase in dimension, a single simulation will require on the order of 1 million normalized CPU hours,

$$500[hrs/k]1000[k/s] \sim 1 \times 10^6 \text{normalized CPU hours.} \tag{105}$$

4.d.3 Timeline

Running this high fidelity transient simulation just one time in 2015 will be a reasonable timeline. The ideal software development timeline for this project is below :

t = Oct-Dec : benchmark the 0D model

t = Oct-Apr : generate cross-sections

t = Dec-Apr : reimplement 0D model as 3D in the MOOSE/PRONGHORN framework

t = Apr-Jun : run low-fidelity testing, benchmark, and scaling studies on Berkelium & BRC-Savio

t = Jun-Oct : Prepare to run full-scale simulation at NERSC

t = Oct-Dec : Potentially run additional parameterized simulations at NERSC? (or, write paper)

5 Available Software

5.a Key Features

The software needed to conduct this work should comply with the guidelines laid out in the FHR Methods and Experiments White Paper. In particular, this software should at least be :

- Capable of pebble bed geometry thermal-fluid analysis and neutronics
- NQA-1 Compliant
- Well-maintained and actively developed

- Cluster-ready
- Validated for FHR applications

5.b Available Tools

Among multiphysics-capable tools that have been benchmarked for pebble bed reactor cores, MOOSE and PARCS lead the field.

5.c MOOSE and PRONGHORN

An open-source multiphysics framework called MOOSE has been developed by Idaho National Laboratory (INL) to conduct fully coupled analyses. This tool can be built upon with custom modules representing various physics. Evaluated cross-sections can be combined with the PRONGHORN module to conduct both steady-state and transient analyses for very high temperature gas-cooled reactors.

The PRONGHORN (PRONGHORN) tool captures porous medium pebble bed thermal-fluid flow as well as diffusion-based neutronic analysis.

5.c.1 Architecture

The MOOSE framework is written in a modern coding language, C++. Additionally, both MOOSE and PRONGHORN are developed using modern programming practices. These libraries are both version controlled and equipped with comprehensive test suites for continuous integration and verification during development.

5.c.2 Geometry

PRONGHORN was initially developed specifically for pebble bed cores. Incorporating the geometry of the PB-FHR is simply a matter of generating the appropriate mesh. This can be done using a number of open source tools. An initial effort to do this using the PyNE tool has already begun.

5.c.3 Neutronics

Cross sections are not generated by PRONGHORN.

5.c.4 Thermal Hydraulics

5.c.5 Materials Performance

5.c.6 Relevant Benchmark Problems

The PBMR400 benchmark problems were conducted with PRONGHORN. The results demonstrate a good match with other codes and promises high fidelity analysis results for a high temperature pebble bed reactor anlaysis.

5.d PARCS

The PARCS tool is capable of mu

5.d.1 Architecture

PARCS is written in FORTRAN-90. While integration testing is incorporated, user experinece has shown that version control and unit testing workflows are omitted during the development of this code.

5.d.2 Geometry

PARCS was developed for advanced reactors in general, and capturing pebble bed core geometry has been added [29]. However, due to the non-modular nature of the code architechture, direct changes to the framework will be necessary in order to model the thermal-fluid behavior in the PB-FHR core.

5.d.3 Relevant Benchmark Problems

The PBMR400 benchmark has been conducted with PARCS as well. PARCS performance was well matched to comparable codes. This result is promising and

5.d.4 HTR LOHS, Brown, Downar et al. [1]

Used THERMIX for thermal hydraulics, PARCS for steady state flux shapes, RELAP5/MOD3.3 for a point kinetic reference point, and used a custom PKE for the neutron kinetics solution.

References

[1] N. R. Brown, V. Seker, S. T. Revankar, and T. J. Downar, "Transient simulation of an endothermic chemical process facility coupled to a high temperature reactor: Model development and validation," *Nuclear Engineering and Design*, vol. 248, pp. 1–13, July 2012.

[2] U. M. Facilitators, M. I. T. Facilitators, and U. B. Facilitators, "Fluoride-Salt-Cooled High Temperature Reactor (FHR) Materials, Fuels and Components White Paper," *Fluoride-salt-cooled High-Temperature Reactor Workshop White Papers*, 2013.

[3] D. L. Krumwiede, C. Andreades, J. Choi, A. Cisneros, L. Huddar, K. D. Huff, M. Laufer, M. Munk, R. O. Scarlat, J. E. Seifried, N. Zwiebaum, E. Greenspan, and P. F. Peterson, "Design of the Mark-1 Pebble-Bed, Fluoride-Salt-Cooled, High-Temperature Reactor Commercial Power Plant," in *Proceedings of ICAPP*, (Charlotte, North Carolina), 2014.

[4] G. I. Bell and S. Glasstone, *Nuclear Reactor Theory*. New York: Van Nostrand Reinhold Company, 1970.

[5] W. M. Stacey, *Nuclear reactor physics*. Wiley. com, 2007.

[6] D. A. Knoll and D. E. Keyes, "Jacobian-free NewtonKrylov methods: a survey of approaches and applications," *Journal of Computational Physics*, vol. 193, pp. 357–397, Jan. 2004.

[7] H. Park, D. Gaston, S. Kadioglu, D. Knoll, R. Martineau, W. Taitano, D. Lebrun-Grandie, and D. Lebrun, "Tightly coupled multiphysics simulation for pebble bed reactors," in *American Nuclear Society 2009 International Conference on Advances in Mathematics, Computational Methods, and Reactor Physics*, 2009.

[8] M. P. Short, B. K. Kendrick, T. Besmann, C. R. Stanek, S. Yip, B. Jones, and J. Henshaw, "Multiphysics Modeling of Porous CRUD Deposits in Nuclear Reactors," *Journal of Nuclear Materials*, vol. 443, no. 1-3, pp. 579–587, 2013.

[9] S. R. Novascone, J. D. Hales, B. W. Spencer, and R. L. Williamson, "Assessment of PCMI Simulation Using the Multidimensional Multiphysics BISON Fuel Performance Code," tech. rep., Idaho National Laboratory (INL), 2012.

[10] S. R. Novascone, R. L. Williamson, J. D. Hales, M. R. Tonks, D. R. Gaston, C. J. Permann, D. Andrs, and R. C. Martineau, "A Multidimensional and Multiphysics Approach to Nuclear Fuel Behavior Simulation," in *PHYSOR 2012 Advances in Reactor Physics Linking Research, Industry, and Education*, (Knoxville, Tennessee, USA), American Nuclear Society, La Grange Park, IL 60526, United States, 2012.

[11] D. Gaston, G. Hansen, S. Kadioglu, D. A. Knoll, C. Newman, H. Park, C. Permann, and W. Taitano, "Parallel multiphysics algorithms and software for computational nuclear engineering," *Journal of Physics: Conference Series*, vol. 180, p. 012012, July 2009.

[12] M. Fratoni, *Development and applications of methodologies for the neutronic design of the Pebble Bed Advanced High Temperature Reactor (PB-AHTR)*. Ph.D. Dissertation, University of California Berkeley, Berkeley, CA, 2008. ISSN:9781109098358.

[13] M. Fratoni, E. Greenspan, and P. F. Peterson, "Neutronic and Depletion Analysis of the PB-AHTR," tech. rep., American Nuclear Society, 555 North Kensington Avenue, La Grange Park, IL 60526 (United States), 2007.

[14] A. Griveau and P. Peterson, "Modeling and Transient Analysis for the Pebble Bed Advanced High Temperature Reactor (PB-AHTR)," *MS Project Report, UCBTH-07-001*, 2007.

[15] S. J. Ball and C. W. Forsberg, "Advanced high-temperature reactor (AHTR) loss-of-forced-circulation accidents," in *2nd International Topic Meeting on High Temperature Reactor Technology, Beijing, China. Paper F*, vol. 7, 2004.

[16] E. D. Blandford and P. F. Peterson, "A buoyantly-driven shutdown rod concept for passive reactivity control of a Fluoride salt-cooled High-temperature Reactor," *Nuclear Engineering and Design*, vol. 262, pp. 600–610, 2013.

[17] R. O. Scarlat, *Design of Complex Systems to Achieve Passive Safety: Natural Circulation Cooling of Liquid Salt Pebble Bed Reactors*. Ph.D. Dissertation, University of California Berkeley, Berkeley, CA, 2012.

[18] A. T. Cisneros, *Pebble Bed Reactors Design Optimization Methods and their Application to the Pebble Bed Fluoride Salt Cooled High Temperature Reactor (PB-FHR)*. PhD thesis, University of California Berkeley, 2013.

[19] A. Niquille, E. Blandford, C. Galvez, and P. Peterson, "MODELING AND TRANSIENT ANALYSIS FOR THE MODULAR PEBBLE-BED ADVANCED HIGH TEMPERATURE," in *Joint International Workshop: Nuclear Technology and Society Needs for Next Generation*, (Berkeley, California), Jan. 2008.

[20] C. Galvez, "Design and Transient Analysis of Passive Safety Cooling Systems for Advanced Nuclear Reactors," *eScholarship*, Jan. 2011.

[21] E. Greenspan, "Thesis Chapter for feedback: PB-FHR Parametric Studies (personal communication)," Dec. 2013.

[22] J. R. Lamarsh and A. J. Baratta, *Introduction to nuclear engineering*, vol. 3. Addison-Wesley Massachusetts, 1975.

[23] Wikipedia, "Lumped capacitance model," Aug. 2014. Page Version ID: 596795944.

[24] J. H. Lienhard V and J. H. Lienhard IV, *A Heat Transfer Textbook: Fourth Edition*. Mineola, N.Y: Dover Publications, fourth edition edition ed., Feb. 2011.

[25] C. Andreades, A. Cisneros, J. Choi, A. Chong, D. L. Krumwiede, L. Huddar, K. D. Huff, M. Laufer, M. Munk, R. O. Scarlat, J. E. Seifried, N. Zwiebaum, E. Greenspan, and P. F. Peterson, "Technical Description of the 'Mark 1' Pebble-Bed, Fluoride-Salt-Cooled, High-Temperature Reactor Power Plant," Thermal Hydraulics Group UCBTH-14-002, University of California, Berkeley, Department of Nuclear Engineering, Berkeley, CA, Sept. 2014.

[26] P. J. Gierszewski and B. B. Mikic, *Property correlations for lithium, sodium, helium, flibe and water in fusion reactor applications*. Massachusetts Institute of Technology, Plasma Fusion Center, 1980.

[27] L. Snead and T. Burchell, "Thermal conductivity degradation of graphites due to nuetron irradiation at low temperature," *Journal of Nuclear Materials*, vol. 224, pp. 222–229, Sept. 1995.

[28] H. Park, D. A. Knoll, D. R. Gaston, and R. C. Martineau, "Tightly coupled multiphysics algorithms for pebble bed reactors," *Nuclear science and engineering*, vol. 166, no. 2, pp. 118–133, 2010.

[29] T. J. Downar, C. Cotton, and T. Kozlowski, "PARCS ACR-700 Reactor Kinetics Modeling," Draft Report Task Order No. 1, Task 3, School of Nuclear Engineering, Purdue University, West Lafayette, IN, United States, May 2005.